

Acidotropic properties of synthetic hexahydropyridoindole antioxidants

Lucia Račková¹ and Marcela Kuniaková²

¹ *Institute of Experimental Pharmacology and Toxicology, Slovak Academy of Sciences, 84104 Bratislava, Slovak Republic*

² *Institute of Medical Biology, Genetics and Clinical Genetics, Faculty of Medicine, Comenius University, 81108, Bratislava, Slovak Republic*

Abstract. In acidic intracellular organelles, sequestration *via* a proton-trapping mechanism is observed for many amine-containing drugs. It may be related to several adverse effects of a drug, yet accumulation of amines bearing antioxidant functionality may provide efficient protection of these compartments. In the present study, a possible proton-trapping mechanism of the novel antioxidant reference stobadine (STO) and its selected derivatives was investigated also with regard to their antioxidant properties, using BV-2 microglia. Unlike its 2-ethoxycarbonyl-8-methoxy derivative EC-STO (pKa₁ 4.95, pKa₂ –3.58), STO, bearing weakly basic piperidine moiety (pKa₂ 9.03), induced vacuolar response in the cells. EC-STO, compared to STO, failed to provide better protection against oxidative damage induced by tert-butyl hydroperoxide (BHP), and that in spite of its predicted improved bioavailability and antioxidant properties. However, disruption of the lysosomal proton gradient abolished the efficacy of STO in suppressing oxidants generation and injury of the cells. NT-STO, the 6-nitro derivative of stobadine, lacking antiradical efficacy, showed a lower effect in protecting the cells against BHP. In conclusion, our study suggests that weakly basic hexahydropyridoindoles may act as lysosomotropic compounds. Furthermore, their weakly basic characteristics may contribute to their improved efficacy in suppressing peroxidative processes within lysosomes, and thus possibly combating ageing-related pathologies.

Key words: Pyridoindoles — Stobadine — Oxidative stress — Free radicals — Lysosomotropy

Introduction

Acidotropic compounds represent an interesting group of substances with application in therapies as well as a probe in cellular biology for assessment of integrity of intracellular acidic vacuoles. Acidotropy is observed for compounds with weakly basic character (pKa ~ 6–10), ensuring their targeting into acidic compartments *via* a proton trapping mechanism (de Duve et al. 1974). In biological systems, acidotropy is typically related to adverse effects giving rise to toxicity of the drugs, as e.g. in the case of the anti-arrhythmic agent amiodarone (Camus and Mehendale 1986; Ammouy et al. 2008) or, on the other hand, to their

therapeutic efficacy (e.g. in the case of the antimalarial drug chloroquine (Yayon et al. 1985)). Intralysosomal accumulation of a drug has less frequently been referred to as beneficial, providing protection against oxidative destabilisation of lysosomes (Dickens et al. 2002; Persson et al. 2003; Kramer et al. 2006). This can be achieved by coupling the weakly basic property of a substance to some antioxidant feature. For instance, propranolol linked to acridine orange was assumed to protect lysosomes against oxidative destabilisation *via* its increased accumulation in acidic compartments (ensured by acridine orange “tag”) and lysosomal iron chelation (ensured by propranolol moiety) (Dickens et al. 2002; Kramer et al. 2006). Persson et al. (2003) introduced 5-[1,2] dithiolan-3-yl-pentanoic acid (2-dimethylamino-ethyl)-amide as another type of lysosomotropic chelator. Vicinal thiols of the reduced form of this compound might interact with intralysosomal iron, thus preventing peroxidative destabilisation of lysosomes

Correspondence to: Lucia Račková, Institute of Experimental Pharmacology and Toxicology, Slovak Academy of Sciences, 84104 Bratislava, Slovak Republic
E-mail: lucia_rackova@hotmail.com

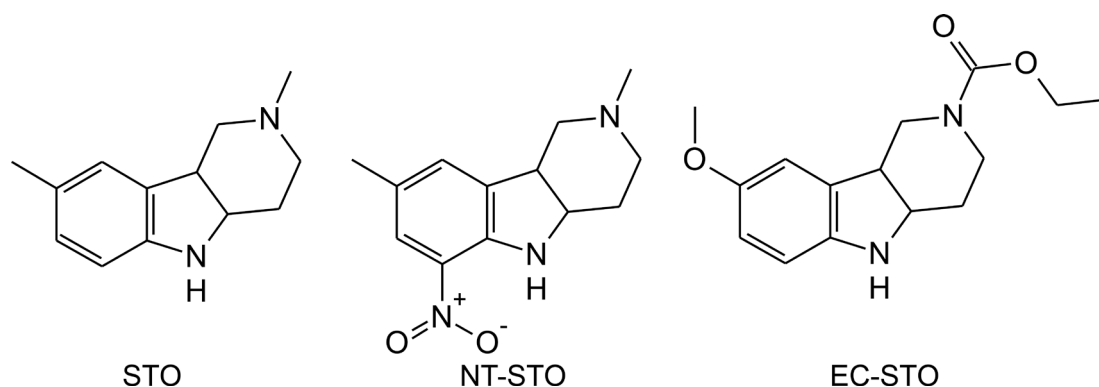


Figure 1. Structures of the hexahydropyridoindoles tested. Stobadine, (-)-cis-2,8-dimethyl-2,3,4,4a,5,9b-hexahydro-1H-pyrido[4,3b]indole (STO), (-)-cis-2,8-dimethyl-6-nitro-2,3,4,4a,5,9b-hexahydro-1H-pyrido[4,3b]indole (NT-STO), (±)-cis-8-methoxy-1,3,4,4a,5,9b-hexahydro-pyrido[4,3-b]indole-2-carboxylic acid ethyl ester (EC-STO).

and subsequent cell damage. More recent work showed that the macrolide antibiotic azithromycin can make lung transplant macrophages and their lysosomes more resistant to oxidant challenge (Persson et al. 2012). On the other hand, lysosomal alkalisation by NH_4Cl was shown to suppress the protective effects of these compounds.

As mirrored by more than two hundred PubMed records, stobadine (STO), (-)-cis-2,8-dimethyl-2,3,4,4a,5,9b-hexahydro-1H-pyrido[4,3b]indole (Fig. 1), is a recognised antioxidant exerting neuroprotective, cardioprotective, anti-hypoxic and anti-arrhythmic effects (Horakova and Stolc 1998). We proposed previously that this compound may represent a promising novel indole-type reference antioxidant (Juránek et al. 2012). Our earlier work also showed that STO and several of its synthetic derivatives efficiently suppressed peroxidation of dioleoyl phosphatidylcholine (DOPC) liposomes (Racková et al. 2006). Quantified by molecular descriptors corresponding to its free radical scavenging capacity and partitioning into the lipid phase, this effect was found to be dependent on the chemical structure of hexahydropyridoindole compounds. In this regard, increased basicity of piperidine nitrogen of STO (as reflected by respective experimental and theoretical value of pKa, 8.5 (Stefek et al. 1989) and 9.02 (MarvinSketch 6.3.1, 2014)) was proposed to counteract its efficient incorporation into the lipid phase due to augmented protonation under physiological conditions. However, its role as a possible trigger of increased accumulation of hexahydropyridoindoles within low-pH intracellular compartments has not been investigated so far.

Oxidative stress plays an important role in ageing of the central nervous system (CNS) and ageing-related neurodegeneration (Mariani et al. 2005). Microglia, as tissue macrophages, represent the main effectors in prooxidant and inflammatory processes in the ageing brain. Under

homeostasis, however, they are involved in a range of physiological processes such as extracellular debris clearance, immune defense, regulation of synaptic activity or tissue repair (Tremblay et al. 2011). The protection of their lysosomal compartment may be of particular relevance in view of increased iron accumulation and a progressive change to a more prooxidant environment during ageing (Wong 2013).

In this study, on using the BV-2 microglia model, we investigated a possible lysosomal trapping mechanism of STO and its selected derivatives also with regard to their antioxidant properties.

Materials and Methods

Chemicals

All reagents were of analytical grade or the highest possible purity.

Thiazolyl blue tetrazolium bromide (MTT), acridine orange, ethidium bromide, 2',7'-dichloro-dihydrofluorescein diacetate and other chemicals were obtained from Sigma-Aldrich, Inc. (Bratislava, Slovakia), unless otherwise stated. JC-1 was obtained from Santa Cruz Biotechnologies Inc. (Heidelberg, Germany).

Stobadine (-)-cis-2,8-dimethyl-2,3,4,4a,5,9b-hexahydro-1H-pyrido[4,3b]indolinium chloride (STO), (-)-cis-2,8-dimethyl-6-nitro-2,3,4,4a,5,9b-hexahydro-1H-pyrido[4,3b]indole (NT-STO) and (±)-cis-8-methoxy-1,3,4,4a,5,9b-hexahydro-pyrido[4,3-b]indole-2-carboxylic acid ethyl ester (EC-STO) (>99.5% purity, GC-MS; Fig. 1) were synthesised at the Institute of Experimental Pharmacology and Toxicology, Slovak Academy of Sciences, Bratislava (Stolc et al. 2003).

Cell culture and administration of the compounds tested

The immortalised mouse microglial cell line BV-2 (developed in the laboratory of Dr. Blasi at the University of Perugia, Italy (Blasi et al. 1990)) was cultured in Dulbecco's Modified Eagle Medium (DMEM), supplemented with 10% FBS (fetal bovine serum) and with 1% P/S (100 U/ml penicillin, 100 µg/ml streptomycin; Biotech Ltd., Bratislava, Slovakia) and maintained in 5% CO₂ at 37°C. Cells were used for 10 passages at maximum. Primary microglia were isolated from the rat brain as described by Guilian and Baker (1986) with few modifications. For the isolation, a 4-week-old Wistar rat (from the breeding station Dobrá Voda, Slovak Republic) was used. The study was performed in compliance with the Principles of Laboratory Animal Care and was approved by the institutional Ethics Committee and by the State Veterinary and Food Administration of the Slovak Republic (Ro-2590/11-221). The animal was kept in an air-conditioned room with 12 h day/night mode and drinking water *ad libitum*. In brief, following the aseptic removal of the brain, blood vessels and membranes were carefully separated. The brain was homogenated and digested (Neural Tissue Dissociation Kit (T), Miltenyi Biotec, Biohem Ltd., Bratislava) and the brain cell suspension was plated in Dulbecco's Modified Eagle Medium/Nutrient Mixture F-12 (DMEM/F12), supplemented with 10% FBS and 1% P/S (100 U/ml penicillin, 100 µg/ml streptomycin; Biotech Ltd., Bratislava, Slovakia). After 11 days, microglial cells were separated by gentle shaking from the underlying astrocytic monolayer. The stock solutions of the substances tested were prepared in distilled water.

Viability assays and microscopy

The cells were grown in 96-well microplates (initial plating density 50.000 cells/well), in complete DMEM. At the end of incubation with the substances tested (24 h or 1 h), the cells were incubated with MTT (0.5 mg/ml) in fresh DMEM in 5% CO₂ at 37°C for 60 min. Subsequently, 80 µl of DMSO was added and the absorbance of dissolved formazan was spectrophotometrically recorded at 570 nm.

Cytotoxicity of tert-butyl hydroperoxide (BHP) to BV-2 cells was assessed by labelling the cells by means of the mixture acridine orange (AO)/ethidium bromide (EB) (Ribble et al. 2005). Briefly, following exposure to the compounds tested and incubation with BHP (5 mmol/l, 1 h, 37°C), the cells were labelled with AO/EB mixture (5 µg/ml : 5 µg/ml) for 30 min at 37°C in full medium. Then the cells were viewed under a Leica DM IL LED fluorescence microscope. Ethidium-bromide-positive cells were counted in 4 independent images at least using the programme Image J (version 1.46r, NIH, <http://rsbweb.nih.gov/ij/>).

Vacuolar response of the cells exposed to basic hexahydropyridoindoles (1 and 5 mmol/l, 2 h) was observed by using Leica DM IL LED light microscope, equipped with integrated Hoffman modulation contrast.

Measurement of intracellular accumulation of the compounds tested

Following the treatment of BV-2 cells (grown overnight at initial plating density of 150.000 cells/cm²) with the compounds tested (2 h, 37°C, at the concentrations of 1 and 3 mmol/l), the incubation medium was removed, the cells were washed with PBS and lysed with the mixture ethanol : 1% acetic acid (1:1). The concentration of the compounds tested in the lysates was calculated using the calibration curves constructed for STO and EC-STO, by application of spectrofluorometry (excitation 230 nm and emission 360 nm for STO; excitation 230 nm and emission 380 nm for EC-STO). The calibration curve for NT-STO was constructed by application of spectrophotometry (with the wavelength set to a maximum at 430 nm).

Assessment of mitochondrial membrane potential

Following treatment of BV-2 cells in 96-well plates (initial plating density 50.000 cells/well) with the compounds tested (1 h, 37°C), the incubation medium was replaced with a fresh medium containing BHP (tert-butyl hydroperoxide; 5 mmol/l, 1 h, 37°C). Subsequently, the cultures were incubated with the freshly prepared JC-1 solution (5 µg/ml) in full DMEM in 5% CO₂ atmosphere at 37°C for 30 min (Roy et al. 2008). After JC-1 was removed, the cells were washed trice with PBS and viewed under a Leica DM IL LED fluorescence microscope. At the same time, the fluorescence was read in a plate reader at excitation 550 nm and emission 600 nm (red fluorescence) and at excitation 485 nm and emission 525 nm (green fluorescence). The red to green fluorescence ratio was evaluated as the parameter of mitochondrial polarisation.

Lysosomal integrity assay

Lysosomal integrity was assessed by the neutral red uptake (NRU) assay (Milackova et al. 2015). Following the treatment of BV-2 cells in 96-well plates with the compounds tested (1 h, 37°C), the incubation medium was replaced by a fresh medium containing BHP (5 mmol/l, 1 h, 37°C). Next, the cultures were incubated with the neutral red (NR) solution (0.006%) in full DMEM in 5% CO₂ atmosphere at 37°C for 30 min. After the NR solution was removed, the cells were washed twice with PBS and solubilised with the mixture ethanol : 1% acetic acid (1:1). After 10 min the absorbance was measured spectrophotometrically at 540 nm using the reference wavelength at 690 nm.

Oxidant production assay

Following the treatment of BV-2 cells in 6-well plates (at initial plating density 150.000 cells/cm²) with the compounds tested (0.5 mmol/l, 1 h, 37°C), the incubation medium was replaced by a fresh medium containing BHP (5 and 10 mmol/l). The higher plating cell density (206.000 cells/cm²) was used for the assay in the plate reader format to avoid loss of cells during treatment (5 mmol/l BHP, 1 h, 37°C). Then the cultures were trypsinised and incubated with the solution of 2',7'-dichloro-dihydrofluorescein diacetate (5 µmol/l) for 30 min in 5% CO₂ atmosphere at 37°C (Halliwell and Whiteman 2004). After the staining solution was removed, the cells were washed with PBS, and analysed by flow cytometry. For assessment of individual samples, a total of 7500-gated events were analysed *per* sample by a flow cytometer (Cytomics FC 500; Beckman Coulter). Alternatively, fluorescence of the oxidation product dichlorofluorescein was read in a plate reader at excitation 488 nm and emission 525 nm.

Proteasomal and lysosomal activity assay

Proteasomal activity was measured as described elsewhere (Rackova et al. 2009). In brief, the equal volumes

of the cell lysate and fluorogenic peptide suc-LLVY-MCA (0.2 mmol/l) were added to the master mix incubation buffer. For determination of the ATP-independent proteasomal activity, 25 µg/ml hexokinase and 15 mmol/l 2-deoxy-D-glucose were added to the incubation mixture. The mixture was incubated for 30 min at 37°C. The fluorescence of the liberated methyl coumarin amide (MCA) was measured at an excitation wavelength of 390 and 460 nm for emission. By using free MCA as standard, the fluorescence values of the reaction product were converted to nanomoles. The lysate was incubated with 15 mmol/l 4-nitrophenyl N-acetyl-β-D-glucosaminide in 0.1 mol/l citrate buffer (pH 4.3) for 30 minutes at 37°C to assess the activity of the lysosomal enzyme N-acetyl-β-D-glucosaminidase (NAG) (Navarova et al. 1999). The reaction was stopped by addition of 0.5 mol/l sodium carbonate buffer (pH 10.5) and the absorption of light by p-nitrophenol released in the reaction was measured at 450 nm. By using a calibration curve for p-nitrophenol, the absorbance values were converted to micromoles of the reaction product.

Fe²⁺ binding capacity assay

The iron binding capacity assay was performed according to the method by Wong and Kitts (2001) with some

Vacuolar response caused by weak bases

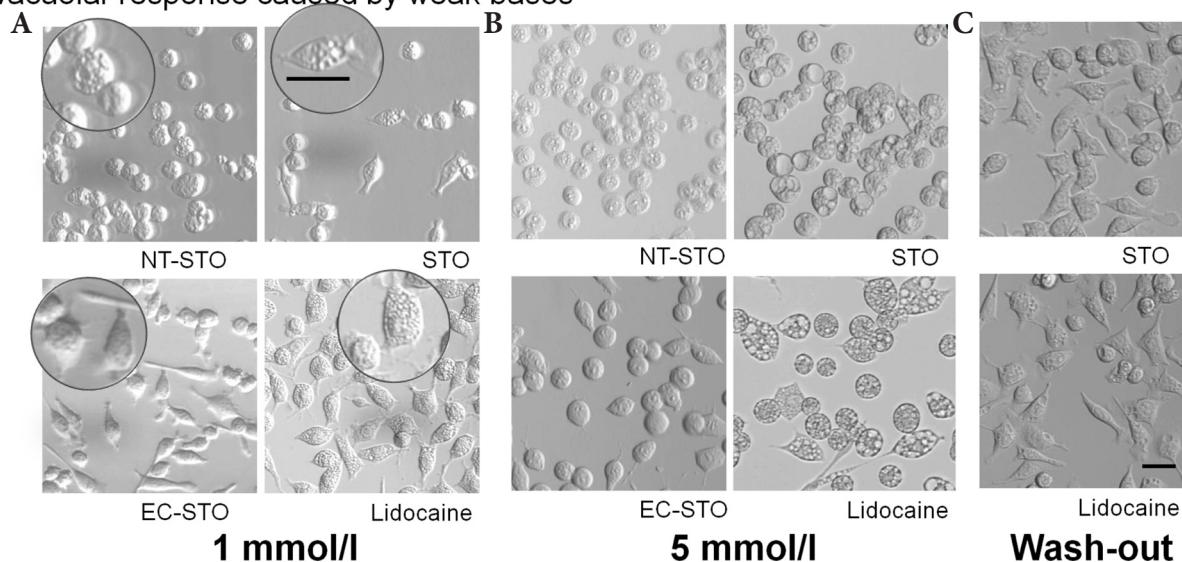


Figure 2. Vacuolar response in microglia exposed to hexahydropyridoindoles tested. BV-2 cells were incubated with NT-STO, STO, EC-STO and the lysosomotropic agent lidocaine for 2 h at 1 mmol/l (A) and 5 mmol/l (B). Small vacuoles were observed using Leica DM IL LED light microscope equipped with integrated Hoffman modulation contrast in the cells exposed to basic hexahydropyridoindoles NT-STO and STO as well as to lidocaine at 1 mmol/l (A). Large vacuoles are induced in the cells exposed to STO and lidocaine (5 mmol/l; B). The cells exposed to NT-STO (5 mmol/l) lack vacuoles due to the increased cytotoxicity at this concentration (see Fig. 4). Vacuolar response in the cells exposed to EC-STO is missing due to its reduced basicity. C. The vacuolar response in the STO- and lidocaine-exposed cells (5 mmol/l) was reversed by wash-out with fresh medium for 2 h. Scale bar 20 µm.

modifications. The solution of $(\text{NH}_4)_2\text{Fe}(\text{SO}_4)_2 \times 6 \text{H}_2\text{O}$ in 0.1 mol/l HCl (final concentration 0.18 mmol/l) was added to a 0.3 ml solution of the compounds tested in ethanol (0.4 mmol/l). The mixtures were vigorously vortexed and allowed to stand for 1 h at room temperature in the dark. After incubation, 0.3 ml of 17 mmol/l BHP in ethanol was added to the mixture and the reaction was incubated for further 5 min. To measure free Fe^{3+} in the solution, 12 μl ammonium thiocyanate (3%) was added and the reaction kept at room temperature for 5 min before reading absorbance at 500 nm.

Statistical analysis

Results are expressed as means \pm standard deviation (SD) from at least three separate experiments. For single comparisons, values for p were calculated using the Student's t -test (Fig. 3). For multiple comparisons, values of p were calculated using one-way ANOVA with Tukey's post-hoc analysis (Figures 7, 8, 9, 10) or Dunnett's post-hoc analysis (Figures 4, 5, 6). Programs PAST v. 2.17c and Minitab 17 Statistical Software were used.

Results

Physico-chemical properties of hexahydropyridoindoles and vacuolar response

Correspondingly to their increased basicities (reflected by the respective calculated $\text{pK}_{\text{a}2}$ values 9.03 and 8.11 for STO and NT-STO (MarvinSketch 6.3.1, 2014) (Table 1)), the cells exposed to either compound tested (at 1 mmol/l concentration) exhibited a formation of small vacuoles within 2 h of incubation (Fig. 2A). Exposure to higher concentrations of the pyridoindoles tested (5 mmol/l) caused formation of large vacuoles in the cells exposed to STO comparable to the effect of lidocaine, a substance with defined lysosomotropic activity (Fig. 2B) (Vandenbroucke-Grauls et al. 1984). This compensatory osmotic response may be due to increased accumulation of the two basic pyridoindoles in acidic vacuoles, as reflected by values of the distribution ratio (DR) 15.6 and 14.2 for STO and NT-STO, respectively. DR, corresponding to equilibrium concentration of a compound within cytosolic (C) vs. lysosomal (L) space, was calculated according to Eq. 1. (Persson et al. 2003):

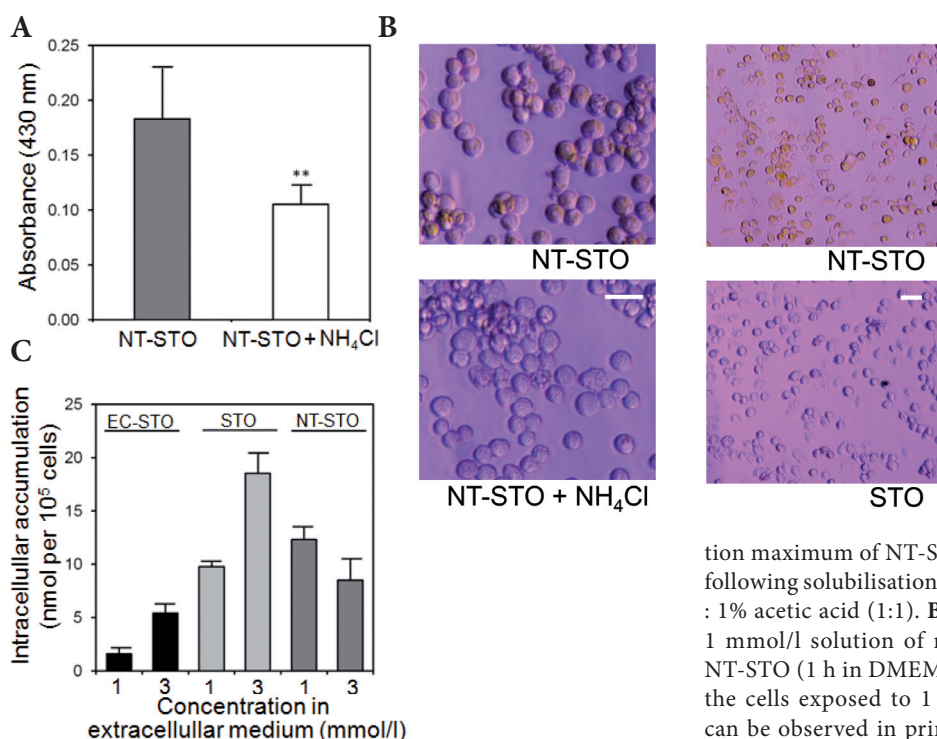


Figure 3. Increased staining of microglia exposed to hexahydropyridoindoles tested. **A.** The increased intracellular incorporation of the red-orange substance NT-STO (1 mmol/l) documented as yellow staining of BV-2 cells (at localisation of the stain mainly in the perinuclear region of the cells). Pre-exposure of BV-2 cells to 10 mmol/l NH_4Cl (15 min) followed by incubation with NT-STO (1 mmol/l) in the continuing presence of 10 mmol/l NH_4Cl suppressed the coloration of cells. The absorbance (at 430 nm corresponding to absorption maximum of NT-STO) was read in plate reader format following solubilisation of the cells with the mixture ethanol : 1% acetic acid (1:1). **B.** Rat primary microglia exposed to 1 mmol/l solution of red-orange hexahydropyridoindole NT-STO (1 h in DMEM) show yellowish coloration (unlike the cells exposed to 1 mmol/l STO). Stronger coloration can be observed in primary cells because of a more abundant number of lysosomes. **C.** Intracellular accumulation

of weakly basic hexahydropyridoindoles STO and NT-STO compared to EC-STO possessing reduced basicity. Following exposure of BV-2 cells to the compounds tested for 2 h, their concentration in the cell lysates was determined using the calibration curves constructed for STO and EC-STO and application of spectrofluorometry. The calibration curve for NT-STO was constructed by application of spectrophotometry (with the wavelength set to maximum at 430 nm). Results represent the mean of 3 experiments \pm S.D. Scale bar 20 μm .

of weakly basic hexahydropyridoindoles STO and NT-STO compared to EC-STO possessing reduced basicity. Following exposure of BV-2 cells to the compounds tested for 2 h, their concentration in the cell lysates was determined using the calibration curves constructed for STO and EC-STO and application of spectrofluorometry. The calibration curve for NT-STO was constructed by application of spectrophotometry (with the wavelength set to maximum at 430 nm). Results represent the mean of 3 experiments \pm S.D. Scale bar 20 μm .

$$DR = [1 + 10^{pK_a - pH(L)}] / [1 + 10^{pK_a - pH(C)}] \quad (1)$$

where pH (C) corresponds to the value of cytosolic pH = 7.2. For lysosomal pH(L), the value 6.0, reported for less acidic microglial lysosomes, was used (Majumdar et al. 2007). However, a vacuolar response was not observed for EC-STO (Fig. 2A, B), which cannot be successively accumulated in the acidic compartments (as reflected by DR 1.08, Table 1). The vacuolar response in the cells exposed to NT-STO at 5 mmol/l concentration was missing in line with its significant toxic effect at this concentration (Fig. 2B, 4B).

In analogy with other lysosomotropic compounds (Hiruma and Hwakami 2011), the vacuolar response in the STO- and lidocaine-exposed cells was reversed by wash-out with fresh medium for two h after a two-h treatment with these weak bases (Fig. 2C).

The increased intracellular incorporation of the red-orange substance NT-STO (1 mmol/l) was documented as yellow staining of both primary microglia and BV-2 cells (at localisation of the stain mainly in the perinuclear region of BV-2 microglia, Fig. 3A) with stronger staining of primary cells in correspondence with their increased number of lysosomes (Fig. 3B). The yellow coloration of BV-2 cells was prevented by pre-incubation with 10 mmol/l NH₄Cl (Fig. 3A), a compound commonly used to disrupt the proton gradient across the lysosomal membrane (Persson et al. 2003), further confirming sequestration of NT-STO (and most likely also of its colourless analogue STO) within acidic vacuoles *via* the proton-trapping mechanism.

Furthermore, unlike EC-STO, both weakly basic pyridindoles NT-STO and STO showed notably enhanced accumulation within the cells (Fig. 3C). Yet again, in analogy with its limited vacuolar response, increased cytotoxicity of NT-STO at the concentration 3 mmol/l may counteract its successive accumulation within acidic vacuoles.

Cytotoxicities of hexahydropyridindoles

Mild comparable diminution of viabilities was observed in the cells incubated with EC-STO and STO for 24 h ($69.7 \pm 2.5\%$ and $63.7 \pm 9.9\%$ viability of control, $p < 0.001$, for 1 mmol/l EC-STO and 1 mmol/l STO, respectively, Fig. 4A). In contrast, the derivative NT-STO showed increased cytotoxicity ($6.2 \pm 0.6\%$ viability of control, $p < 0.001$ at 1 mmol/l concentration). Lidocaine, a compound reported for its lysosomotropic effect (Vandenbroucke-Grauls et al. 1984), showed a mildly lower cytotoxic effect than did STO and NT-STO ($82.6 \pm 2.4\%$ of control, $p < 0.05$, at 1 mmol/l concentration). The viabilities of the cells exposed to the compounds tested at 1 mmol/l concentration were not influenced within a 2-h incubation time. However, the higher concentrations of the compounds tested (used for the examination of vacuolar effect) showed cytotoxicities in the order: NT-STO > STO > EC-STO > Lidocaine (Fig. 4B).

Effect of hexahydropyridindoles on proteolytic activities

None of the hexahydropyridindoles tested (at 0.1 mmol/l concentration and 24 h exposure) influenced the activity of the lysosomal enzyme N-acetyl- β -D-glucosaminidase (NAG) (Fig. 5A). Yet both ATP-dependent and -independent proteasomal activities were diminished in the treated cells (Fig. 5B), with the most significant effect of NT-STO (0.250 ± 0.037 nmol·mg⁻¹·min⁻¹, $p < 0.01$, and 0.278 ± 0.002 nmol·mg⁻¹·min⁻¹, $p < 0.01$, for 26S+20S and 20S proteasomal activity, respectively, compared to 0.489 ± 0.009 nmol·mg⁻¹·min⁻¹ and 0.387 ± 0.025 nmol·mg⁻¹·min⁻¹ for 26S+20S and 20S proteasomal activity, respectively, in control cells). In addition, within 6 h of incubation, increased autofluorescence was seen in the cells incubated with the non-fluorescent pyridindole NT-STO (Fig. 5C).

Table 1. Physico-chemical properties of hexahydropyridindoles tested

	pK _{a1} ^a	pK _{a2} ^a	logP ^a	logP ^{'a}	$-\Delta A/\Delta t$ (s ⁻¹) ^b	DR ^c	P-gp (substrate) ^d
STO	2.53 (3.2)*	9.03 (8.5)*	1.95	1.63	0.012 ± 0.002	15.6	0.3 (non-substrate)
NT-STO	-1.85	8.11	2.15	2.22	<0.001	14.2	0.28 (non-substrate)
EC-STO	4.95	-3.58	1.79	1.83	0.041 ± 0.002	1.08	0.3 (probably non-substrate)

^a Values of (log P) and pK_a were calculated using the programme Pallas (CompuDrug International; Pallas Version 3.1.1.2). K_{a1} is acid dissociation constant of indolic nitrogen, K_{a2} corresponds to piperidine nitrogen. *Values of pK_a in brackets correspond to experimental values determined for STO (Stefek et al. 1989). Additionally, partition coefficients were calculated by the programme MarvinSketch software (ChemAxon) (logP[']) (MarvinSketch 6.3.1, 2014). ^b Antiradical reactivity ($-\Delta A/\Delta t$) was evaluated as initial rate of absorbance decrease of reaction mixtures of DPPH and the compound tested (Račková et al. 2006, 2011). ^c Distribution ratio (DR) within cytosolic vs. lysosomal space was calculated according to Eq. (1) (see Results), where pH (C) corresponds to the value of cytosolic pH = 7.2 (Persson et al. 2003). For lysosomal pH (L), a value reported for microglial lysosomes was used (Majumdar et al. 2007). ^d P-gp substrate probabilities were calculated using the programme ACD/Labs I-Lab 2.0 (ilab.acdlabs.com).

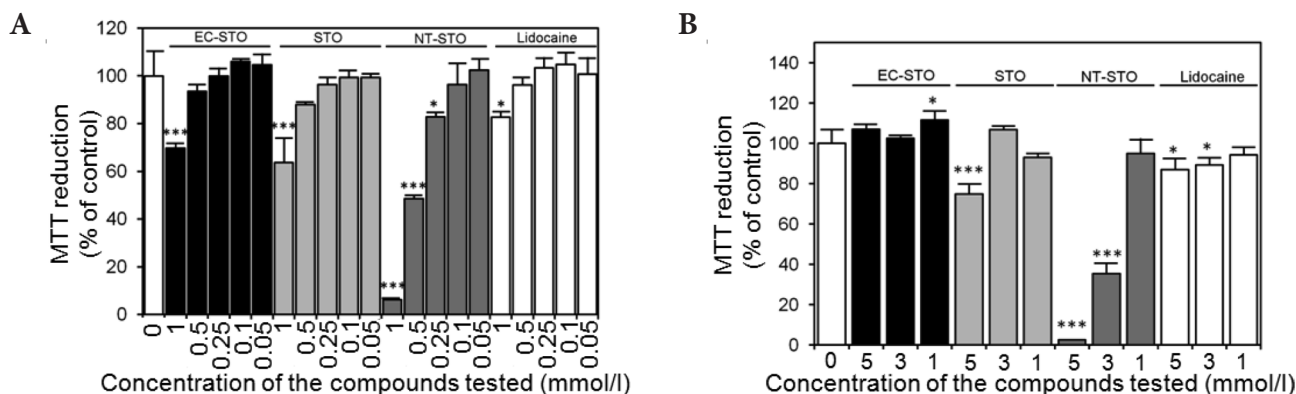


Figure 4. Cytotoxicity effects of hexahydropyridoindoles tested in BV-2 microglia. The cells were incubated with the compounds tested for 24 h (A) or 1 h (B) followed by incubation with MTT (0.5 mg/ml, 1 h) as described in Materials and Methods. Results represent the mean of 3 experiments \pm S.D., * $p < 0.05$, *** $p < 0.001$ vs. control.

Iron-chelating properties of hexahydropyridoindole compounds

None of the hexahydropyridoindoles tested (at 0.2 mmol/l concentration) showed Fe^{2+} binding activity measured by a modified ferric-thiocyanate method (Fig. 6; Wong and Kits 2001). In contrast, the well-known iron chelator ethylenediaminetetraacetic acid (EDTA, 0.2 mmol/l), abolished

the formation of red coloured ferric-thiocyanate complexes arising from oxidation of unbound Fe^{2+} by BHP.

Acidotropic properties and antioxidant efficacies of hexahydropyridoindoles

In order to assess the protective efficacy of the hexahydropyridoindoles tested against oxidative challenge in

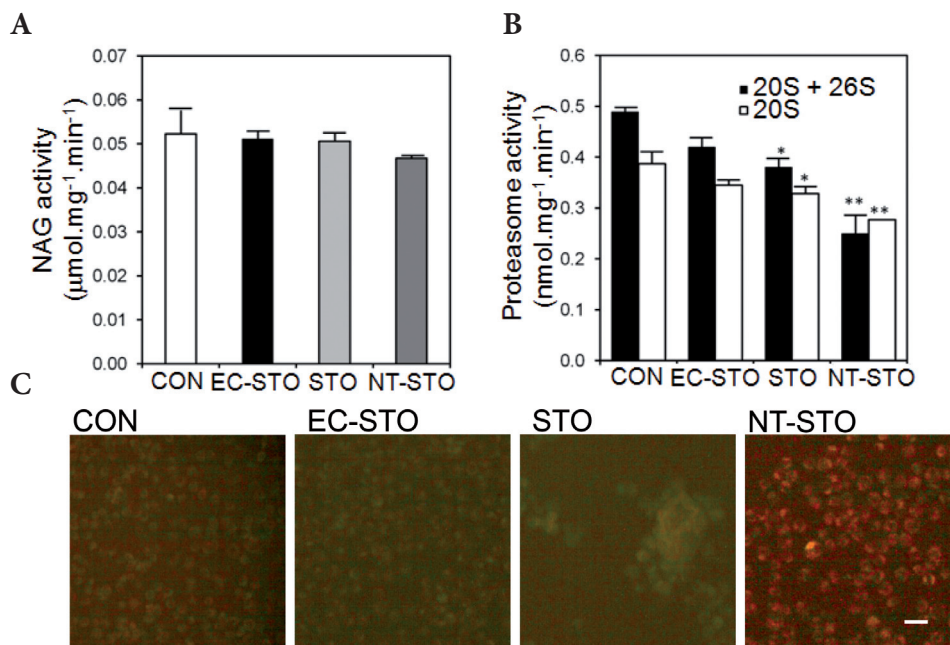


Figure 5. Autofluorescence and proteolytic activity in BV-2 cells exposed to hexahydropyridoindoles tested. A. None of the hexahydropyridoindoles tested influenced the activity of lysosomal enzyme N-acetyl- β -D-glucosaminidase (NAG). B. Both ATP-dependent and -independent proteasomal activities were diminished in the treated cells (at 0.1 mmol/l concentration and 24-h exposure), with NT-STO exhibiting the most significant effect. C. Unlike STO- and EC-STO-treated cells, the cells incubated with NT-STO (6 h, 1 mmol/l) show increased autofluorescence observed under the green channel. Scale bar 20 μm . Results represent the mean of 3 experiments \pm S.D., * $p < 0.05$, ** $p < 0.01$ vs. control (CON).

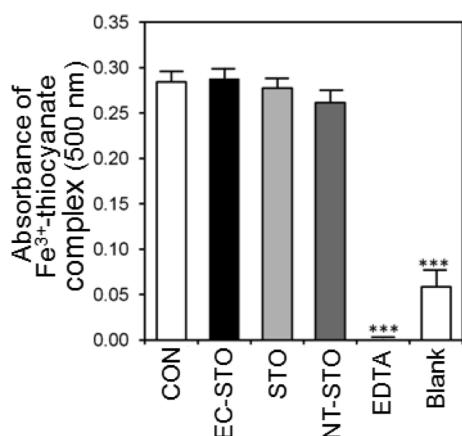


Figure 6. Fe²⁺ binding capacity of hexahydropyridoindoles tested assessed by a modified ferric-thiocyanate method (as described in Materials and Methods). Ethylene diamine tetracetic acid (EDTA) was used as a standard. Results represent the mean of 3 experiments \pm S.D. *** $p < 0.001$ vs. control (CON).

view of their differential intracellular incorporation, the cells were pre-loaded with the substances tested, prior to exposure to BHP in a fresh medium. Exposure of the cells to BHP resulted in a significantly increased accumulation of intracellular reactive oxygen species (ROS) as documented by intracellular oxidation of 2',7'-dichlorodihydrofluorescein diacetate (H₂DCF-DA) followed by flow cytometric analysis (5 and 10 mmol/l BHP; Fig. 7A) and by fluorometry in a plate reader format (5 mmol/l BHP; at higher cell density, Fig. 7B).

Pre-loading with EC-STO and STO suppressed ROS production in the cells exposed to different levels of oxidative stress followed by flow cytometry with rather comparable efficacies at both concentrations of BHP (Fig. 7A). However, NT-STO showed only mild non-significant suppression of ROS generation induced by 5 mmol/l BHP (164 ± 14.1 M.F.I. (mean fluorescence intensity), $p > 0.05$) and no efficacy of NT-STO was observed at 10 mmol/l BHP (260 ± 12.7 M.F.I., $p > 0.05$).

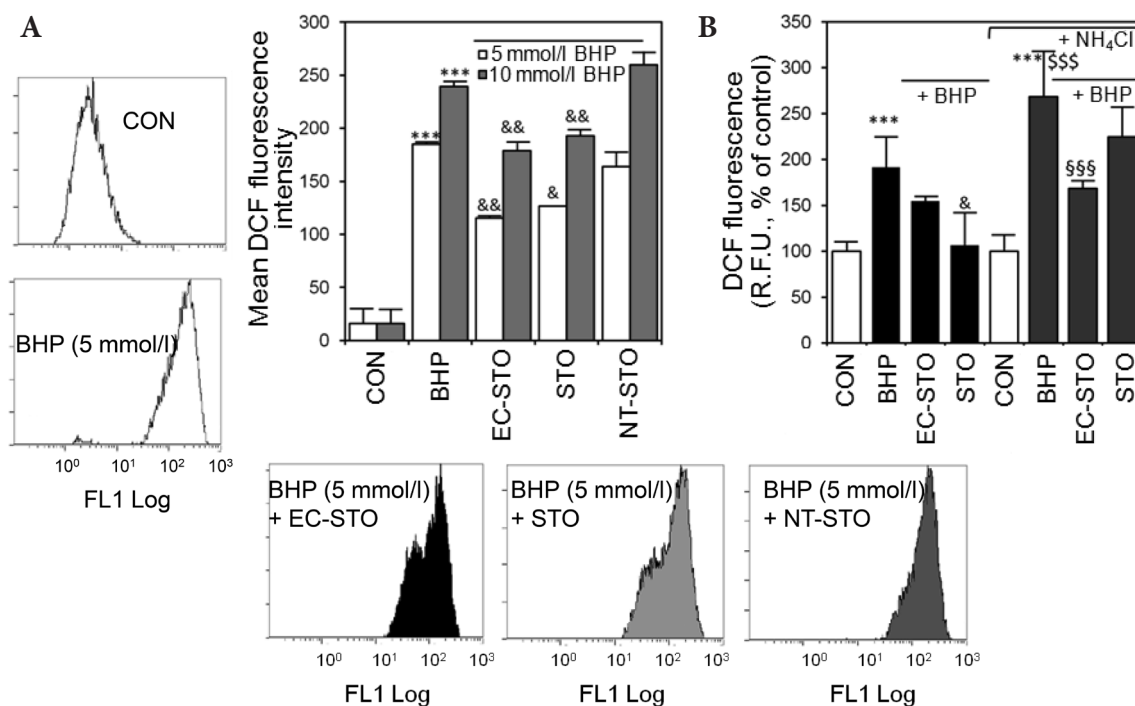


Figure 7. Suppression of oxidative stress by hexahydropyridoindole antioxidants and effect of pH gradient changes. **A.** The cells were pre-loaded with STO, EC-STO and NT-STO (0.5 mmol/l, 1 h) followed by exposure to tert-butylhydroperoxide (BHP; 5 and 10 mmol/l, 1 h). Next, the cells were trypsinised, incubated with dihydro-dichlorofluorescein diacetate (H₂DCF-DA, 5 μ mol/l) and the samples were analysed by flow cytometry as described in Materials and Methods. **B.** Alternatively, the cells were grown in 96-well plates at higher plating density, pre-loaded with STO and EC-STO (0.1 mmol/l, 1 h) followed by exposure to BHP (5 mmol/l, 1 h) and incubation with (H₂DCF-DA, 5 μ mol/l). Fluorescence was analysed in a plate reader. In parallel experiments, BV-2 cells were pre-exposed to 10 mmol/l NH₄Cl (15 min) followed by incubation with STO and EC-STO (0.1 mmol/l) in the continuing presence of 10 mmol/l NH₄Cl. Disruption of proton gradient inverted efficacies of STO and EC-STO against BHP-induced ROS generation. Results represent the mean of 3 experiments \pm S.D., *** $p < 0.001$ vs. control (CON); & $p < 0.05$, && $p < 0.01$ vs. BHP-treated cells; \$\$\$ $p < 0.001$ vs. cells non-treated with NH₄Cl, \$\$\$\$ $p < 0.001$ vs. (BHP+NH₄Cl)-treated cells. R.F.U., relative fluorescence unit.

In addition, pre-loading with STO showed a somewhat better efficacy than with EC-STO in suppressing ROS production followed in plate reader format (with reduced washing procedures, most likely enabling better retention of the sequestered substances; $155 \pm 5.22\%$ R.F.U. (relative fluorescence units) of control, $p > 0.05$, and $107 \pm 35.7\%$ R.F.U. of control, $p < 0.05$, for the cells pre-treated with EC-STO and STO, respectively, vs. $192 \pm 33.7\%$ R.F.U. of control for BHP-treated cells). Disruption of lysosomal proton gradient with 10 mmol/l NH_4Cl led to enhanced generation of ROS in the cells treated with BHP ($269 \pm 48.7\%$ R.F.U. of control, $p < 0.001$ vs. cells treated with BHP only, Fig. 7B). Co-incubation of STO and EC-STO with NH_4Cl eliminated the efficacy of STO in suppressing BHP-induced ROS generation ($169 \pm 8.69\%$, $p < 0.001$ and $225 \pm 33.2\%$ R.F.U. of control, $p > 0.05$ for EC-STO and STO, respectively, Fig. 7B).

Protection by hexahydropyridoindoles against oxidative damage

Incubation of BV-2 microglia with BHP (5 mmol/l) caused a strong depolarisation of mitochondrial membrane potential (documented by reduction of JC-1 dye aggregation in polarised mitochondria and a corresponding decrease of red-to-green fluorescence ratio, $43.3 \pm 9.7\%$ of control

cells, $p < 0.001$, Fig. 8) and a significant lysosomal rupture (confirmed by reduction of neutral red uptake by acidic vacuoles, as well as a corresponding decrease of absorbance of the solubilised entrapped dye, $55.4 \pm 4.29\%$ of control cells, $p < 0.001$, Fig. 9). This was accompanied by a significant increase in the number of ethidium-bromide-positive cells ($57.1 \pm 2.59\%$ vs. $1.57 \pm 1.56\%$ in control cells, $p < 0.001$) and of cells with bright green nuclei and nuclear fragmentation pointing to apoptosis induction (Fig. 10).

Pre-loading with STO and EC-STO at 1 mmol/l concentration resulted in a comparable prevention of BHP damage, as shown by protection of mitochondrial membrane potential, documented by the values of JC-1 red-to-green fluorescence ratio, $76.3 \pm 14\%$ of control, $p < 0.001$ for the cells preloaded with 1 mmol/l EC-STO and $80.7 \pm 16.3\%$ of control, $p < 0.001$, for the cells pre-loaded with STO (Fig. 8). Similarly did pre-loading with STO and EC-STO prevent with comparable efficacy lysosomal rupture (documented as protection of neutral red uptake). A similar protection was observed also at lower concentrations of each compound tested (Fig. 9). In contrast, pre-loading with NT-STO did not protect mitochondrial membrane potential ($51.0 \pm 15.0\%$ of control, $p > 0.05$, at 1 mmol/l concentration) and exerted only mild non-significant protection of neutral red uptake ($72.0 \pm 4.47\%$ of control, $p > 0.05$, Fig. 8, 9).

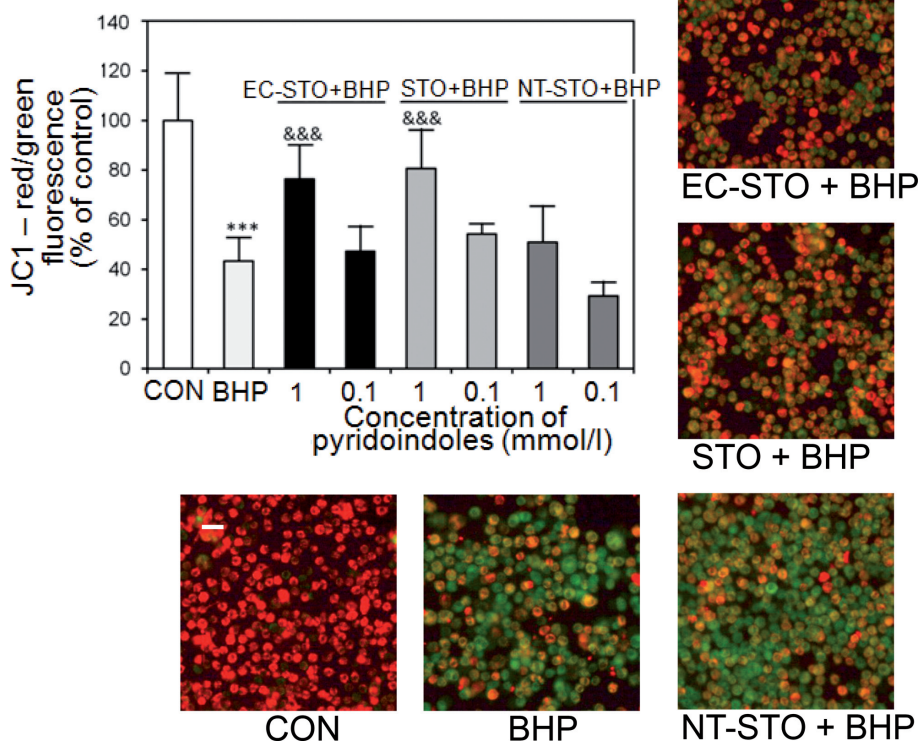


Figure 8. Protective effect of hexahydropyridoindole antioxidants on mitochondrial membrane depolarisation of BV-2 microglia induced by tert-butylhydroperoxide (BHP). The cells were pre-loaded with EC-STO, STO and NT-STO (0.1 and 1 mmol/l, 1 h) followed by exposure to BHP (5 mmol/l, 1 h). Then the cells were incubated with JC-1 (5 μg/ml) as described in Materials and Methods. The ratio red (550/600 nm) to green (485/525 nm) fluorescence was evaluated as a parameter of mitochondrial membrane polarisation. Images show loss of JC-1 aggregation (shown as increase of green fluorescence) due to mitochondrial membrane potential decrease and partial protection by EC-STO and STO (0.5 mmol/l) and lack of protection by NT-STO (0.5 mmol/l); Scale bar 50 μm. Results represent the mean of 4 experiments \pm S.D., *** $p < 0.001$ vs. control; &&& $p < 0.001$ vs. BHP-treated cells.

Pre-loading with STO and EC-STO at 1 mmol/l concentration prevented also with similar efficacy death of cells exposed to BHP, as shown by reduction of EB-positive cells (Fig. 10). Pre-loading with NT-STO showed the least yet still significant diminution of EB-positive cells ($31.7 \pm 10.2\%$ of control, $p < 0.001$). However, in contrast to the effect of STO and EC-STO, the influence of NT-STO on the number of the bright-green-nuclei-positive cells was lower (Fig. 10A).

Disruption of lysosomal proton gradient with 10 mmol/l NH_4Cl mildly diminished the number of EB-positive cells caused by BHP treatment ($42.3 \pm 4.52\%$ vs. $57.2 \pm 2.59\%$ for the cells treated with BHP only, $p < 0.001$, Fig. 10B). Co-incubation of STO and EC-STO with NH_4Cl decreased the efficacy of STO only in reduction of the number of EB-positive cells ($3.2 \pm 1.94\%$, $p < 0.001$ and $26.6 \pm 12.2\%$, $p > 0.05$ for EC-STO and STO, respectively, Fig. 10B). In addition, the protective efficacy of NT-STO against BHP-induced cell death was also reduced following treatment with NH_4Cl ($47.7 \pm 13.0\%$, $p > 0.05$).

Discussion

Increased accumulation in intracellular acidic compartments (such as lysosomes or late endosomes) was reported for

a number of drugs with a structure of primary, secondary and tertiary amines. In spite of their diverse therapeutic targets, the unifying mechanism underlying this phenomenon (defined as „lysosomotropy“ or more precisely „acidotropy“ (de Duve et al. 1974)) depends exclusively on physico-chemical properties of a compound and the existence of lysosomal pH gradient maintained by proton-pump vacuolar ATPase. The mechanism was first described in 1974 by Christian De Duve for lipophilic amines such as chloroquine and neutral red (de Duve et al. 1974). Once an unprotonated form of a weakly basic amine-containing drug enters acidic compartments, it undergoes protonation, after which it can no longer traverse the lipid bilayers of membranes and is therefore “trapped” by these acidic organelles. Consequently, osmotic swelling of the vacuoles occurs due to increased sequestration of a cationic drug. Like all autophagosomes, the amine-induced vacuoles have been suggested to evolve towards lysosomes (Marceau et al. 2012). They were shown to be positive for the late endosome/lysosome markers Rab7 and CD63, the autophagosomal marker LC3-II and the lysosomal marker LAMP-1. The presence of Golgi p230 and golgin-97 indicated that they originated at least in part from trans-Golgi. Autophagolysosome formation may be responsible for the late presence of amorphous material in large vacuoles induced by amines. A prevailing autophagolysosome identity

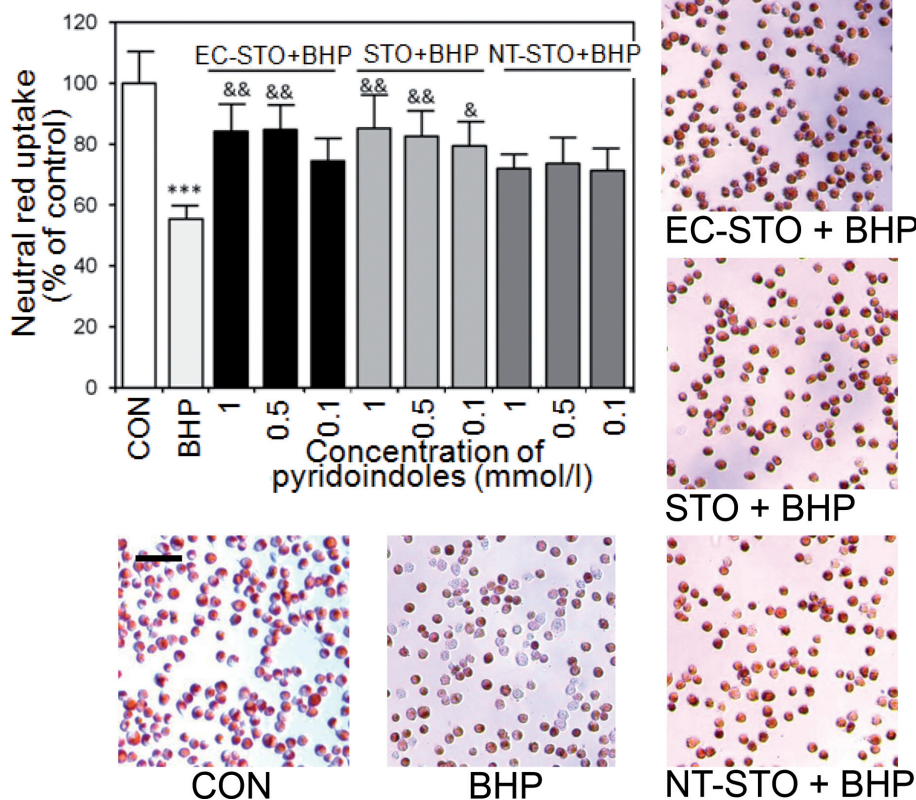


Figure 9. Protective effect of hexahydropyridoindole antioxidants on lysosomal integrity of BV-2 microglia induced by tert-butylhydroperoxide (BHP). The cells were pre-loaded with EC-STO, STO and NT-STO (0.1–1 mmol/l, 1 h) followed by exposure to BHP (5 mmol/l, 1 h). Then the cells were incubated with neutral red (0.006%) as described in Materials and Methods. Neutral red uptake by acidic vacuoles and corresponding absorbance of the solubilised entrapped dye were evaluated in a plate reader at 540 nm using the reference wavelength at 690 nm. Scale bar 50 μm . Results represent the mean of 4 experiments \pm S.D., *** $p < 0.001$ vs. control; && $p < 0.01$, & $p < 0.05$ vs. BHP-treated cells.

of amine-induced vacuoles was confirmed in cancer cell lines transduced with an acid-sensitive green fluorescent protein (Mei et al. 2014).

Logically, successful accumulation of a drug depends mostly on its membrane permeability properties, best reflected by the partition coefficient. In this regard, formation of large vacuoles was evidenced in the cells exposed to drugs with a large value of the partition coefficients $\log P$, such as amiodarone or quinacrine at a micromolar concentration range: $\log P$ 7.9 and 5.67, respectively (Marceau et al. 2012). However, the rather mild vacuolar response observed in the cells exposed to the hexahydropyridoindoles STO and NT-STO corresponded to their moderate lipophilicities with respective $\log P$ 1.95 and 2.15, coupled with enhanced basicities (pK_a 9.03 and 8.11, respectively). For comparison, a vacuolar response was reported also for lidocaine ($\log P$ 2.63, pK_a 7.75 (MarvinSketch 6.3.1, 2014)) at $>$ or $=$ 1 mmol/l concentration in cell culture conditions (Marceau et al. 2012). In this regard, comparable vacuoles were induced by lidocaine and STO at 5 mmol/l concentration. In contrast, lack of vacuolar response in the cells exposed to EC-STO up to 5 mmol/l concentration corresponds to its diminished basicity. However, missing vacuolar swelling in

the cells treated with NT-STO at the higher concentration used corresponds to its increased mitochondrial toxicity (confirmed by MTT assay) that may counteract the function of V-ATPase and thus disturb the lysosomal proton gradient.

Calculated probabilities of the active transport (Table 1) as well as the results of colorimetric and fluorimetric uptake assays of the derivatives of STO (Fig. 3A–C) suggest that accumulation of the basic hexahydropyridoindoles tested within the cells may be governed principally by a physico-chemical process.

Increase of intralysosomal deposition of protein and lipid material as a consequence of perturbation of autophagic flux is one of the main effects of weakly basic drugs (Marceau et al. 2012; Ashoor et al. 2013). Moreover, perturbations in the flux through autophagy have been reported to affect the activity of the ubiquitin proteasome system (UPS) and a number of mechanisms have been proposed to rationalise the link between the UPS and autophagy (Korolchuk et al. 2010). Although the activity of the lysosomal enzyme NAG was not affected by the compounds tested in the assay conditions, lysosomal alkalinisation can decrease its intracellular proteolytic activity. Lysosomal dysfunction can in turn be

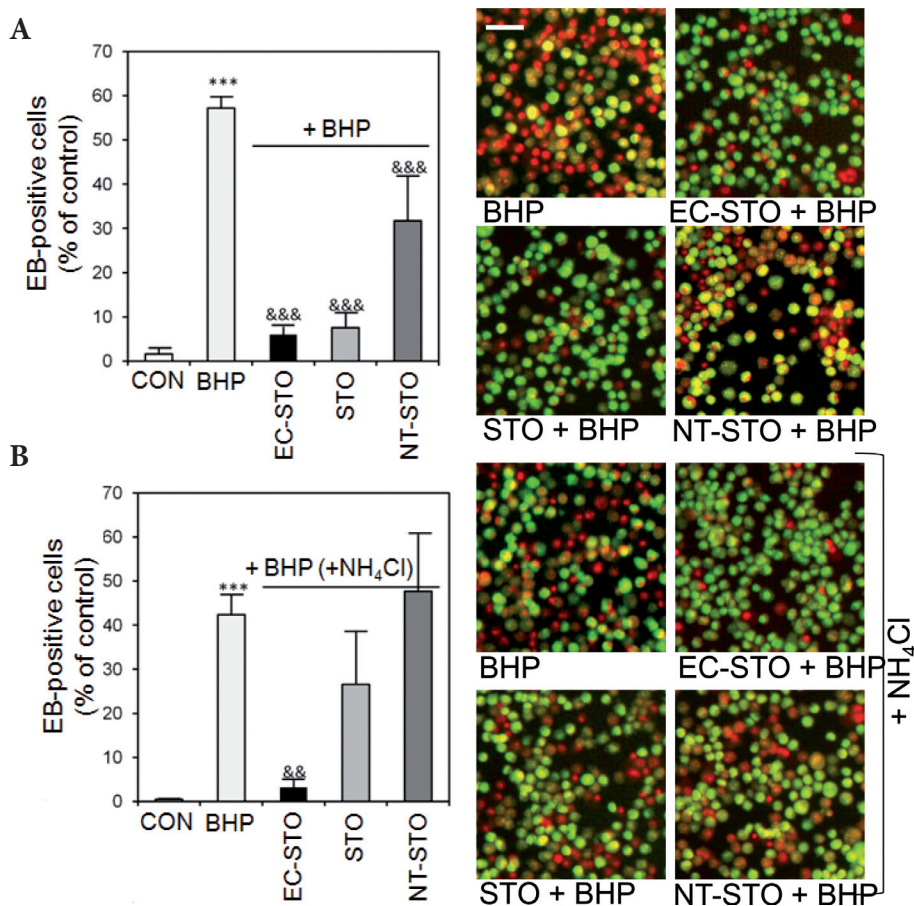


Figure 10. A. Protective effect of hexahydropyridoindole antioxidants on cell death of BV-2 microglia induced by tert-butylhydroperoxide (BHP). The cells were pre-loaded with EC-STO, STO and NT-STO (1 mmol/l, 1 h) followed by exposure to BHP (5 mmol/l, 1 h). Then the cells were incubated with acridine orange/ethidium bromide mixture as described in Materials and Methods. **B.** In parallel experiments, BV-2 cells were pre-exposed to 10 mmol/l NH_4Cl (15 min) followed by incubation with the compounds tested (1 mmol/l) in the continuing presence of 10 mmol/l NH_4Cl . Disruption of proton gradient suppressed efficacies of STO and NT-STO against BHP-induced cell death. Ethidium bromide-positive cells were counted in at least 4 independent images; Scale bar 50 μm . Results represent the mean of 4 images \pm S.D., *** $p < 0.001$ vs. control; && $p < 0.01$, &&& $p < 0.001$ vs. BHP-treated cells.

responsible for the observed decrease of proteasomal activity in NT-STO- and STO-treated cells. Increased accumulation and aggregation of ubiquitinated proteins, reported as the result of autophagy inactivation (Korolchuk et al. 2010), may be also a trigger of proteasomal inhibition (Höhn et al. 2011). In this regard, although other reasons may be associated with increased autofluorescence in NT-STO-treated cells (such as metabolic NADH/NADPH changes or accumulation of a fluorescent metabolite), one might speculate that it could be caused by formation of lipofuscin (accumulated highly cross-linked undegradable autofluorescent aggregate), known to be accelerated by increased lysosomal pH and intra-lysosomal oxidation of auto- and heterophagocytosed material (Sundelin and Terman 2002). In addition, impairment of autophagy flux can lead also to enhancement of cytosolic lipofuscin accumulation (Höhn and Grune 2013). However, autofluorescence was not observed in the cells exposed to the other basic hexahydropyridindole, STO. Prominent antioxidant properties of STO, documented by a range of studies (Juránek et al. 2012) and also previously shown by reactivity with DPPH, Table 1 (Racková et al. 2006), which are interfering with cytosolic and intra-lysosomal oxidative processes may provide a plausible explanation for the lack of autofluorescence. In contrast, a negligible antioxidant capacity can be attributed to NT-STO: $-\Delta A/\Delta t < 0.001$ (Racková et al. 2006), which is most likely to give rise also to a more profound proteasomal inhibition.

Generally, mild cytotoxicity effects can be observed in cultured cells exposed to lysosomotropic drugs over 24 h, a phenomenon related to mitosis arrest, vesicular transport inhibition and autophagic accumulation (Marceau et al. 2012). Several lipophilic cationic drugs (such as chloroquine) exert enhanced cytotoxicities (Jiang et al. 2008). These could be related to additional sequestration of a compound into other subcellular compartments such as mitochondria and nucleus (Jiang et al. 2008; Marceau et al. 2012). In line with its moderate lipophilicity (as reflected by logP value, Table 1), only a mild influence on viability was observed in the cells incubated with STO over 24 h. The cytotoxicity of STO was comparable with the effect of the local anaesthetic lidocaine (logP 2.63). For comparison, adverse effects of lidocaine in patients were reported only at concentrations ≥ 42 mmol/l (corresponding to topical applications) (Hoss et al. 1999). In contrast, NT-STO showed relatively increased cytotoxicity in BV-2 cells. With regard to its moderate lipophilicity, the cytotoxicity of NT-STO is less likely to be related to lysosomal accumulation only or to increased sequestration in other charged subcellular compartments such as mitochondria. For comparison, only an isolated effect of accumulation in the acidic vacuoles was previously observed for the less lipophilic antiarrhythmic drug procainamide (logP 1.13) (Marceau et al. 2012).

As mentioned in Introduction, increased sequestration of a compound ameliorating oxidative stress in acidic vacuoles can represent a favourable mechanism of protection of these compartments. With regard to the importance of postmitotic cells in organism maintenance, mitochondria and lysosomes have been proposed to play the central role in ageing of the whole organism (Brunk and Terman 2002). Mitochondrial and lysosomal age-related alterations may amplify each other, eventually causing profound dysfunction and death of cells. Lysosomes (sensitised to oxidative damage by accumulated lipofuscin sequestering redox-active iron) represent the main target of ROS increasingly generated by defective senescent mitochondria (persisting due to diminished autophagocytosis). Oxidative damage to the lysosomal membrane can eventually lead to its rupture, leakage of lytic enzymes into cytosol, which in turn can damage mitochondria, initiating ultimately the cell death programme. Thus, interference with these vicious cycles can represent a favourable strategy for combating ageing-related pathologies. In spite of their robust mitotic potential, protection of the lysosomal compartments may be of particular relevance in microglia, the resident immune cells of the CNS. Their ageing has been shown to be accompanied by increasing iron load (possibly augmenting intra-lysosomal Fenton-type reactions), lipofuscin sequestration within lysosomes, mitochondrial over-production of ROS coupled to telomere attrition, and eventually to replicative senescence (Wong 2013). Progressive development of a more prooxidant environment can be also associated with an increased activation profile of these immune effector cells during ageing. In addition, the brain has a relatively limited capacity to resupply microglia. Consequently, their premature depletion would probably handicap the physiological processes in the brain controlled by these cells (Liu et al. 2001).

Previous results from a model of peroxidation of DOPC liposomes induced by a water-soluble azo-initiator showed that hexahydropyridindole antioxidants can act as potent scavengers of peroxy radicals both in aqueous and lipid phases (Racková et al. 2002, 2011). In addition, STO was shown to suppress Cu^{2+} -mediated low-density lipoprotein oxidation (Horáková et al. 1996) as well as Cu^{2+} /BHP-induced peroxidation of egg yolk phosphatidylcholine liposomes (Gallová and Szalayová 2004). Increased basicity of nitrogen of the condensed piperidine ring of a hexahydropyridindole (giving rise to its enhanced protonation at physiological pH) was proposed as a property hampering its efficient incorporation into the lipid phase (Racková et al. 2002, 2011). Consequently reduced availability of one of these scavengers within the membrane interior has been suggested to reduce its efficiency in suppression of propagation of lipid peroxidation (Racková et al. 2006, 2011). However, the increased basicity of piperidine nitrogen can be also regarded as a driving force in targeting these antioxidants into

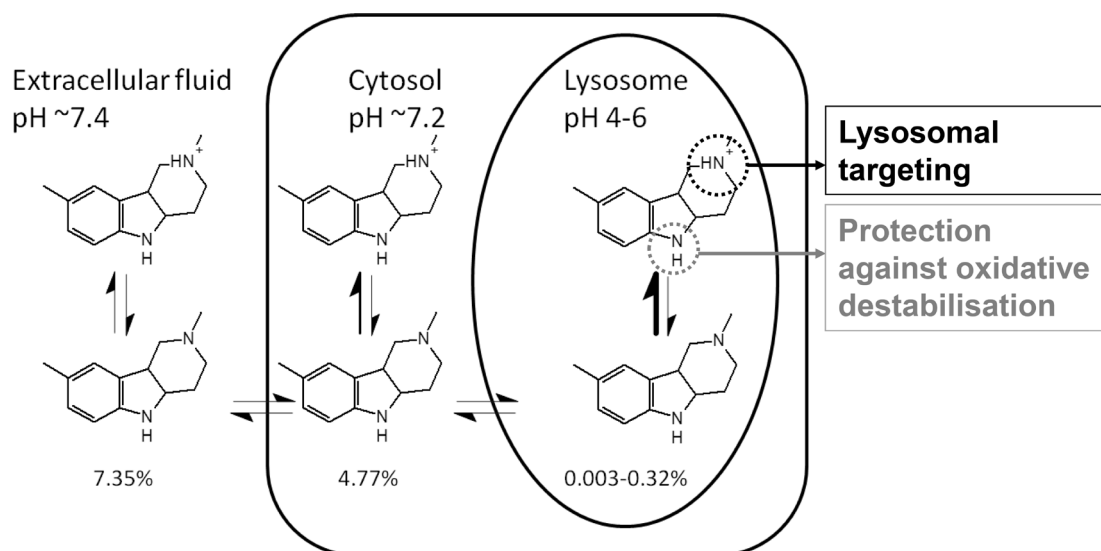
acidic lysosomal compartments. As a result, the accumulated weakly basic hexahydropyridoindoles can efficiently interfere with radicals (either in aqueous phase or at membrane-water interface) derived from Fenton-type reaction catalysed by the sequestered iron. In addition, as supported by previous studies, STO could hinder also intralysosomal Fenton system-induced crosslinking reactions (Kyselova et al. 2003) as well as glycation of proteins (Stefek et al. 1996), the main mechanisms involved in lipofuscin formation. On the other hand, as supported by our present results, protection of lysosomes by hexahydropyridoindoles is not likely to involve chelation of lysosomal redox-active iron.

Peroxidative destabilisation of lysosomes was shown in J774 macrophages following exposure to hydrogen peroxide (Persson et al. 2003; Yu et al. 2003). Tert-butyl hydroperoxide, generally considered a source of lipophilic tert-butyl peroxide radicals and reported as an inducer of mitochondrial generation of $O_2^{\cdot-}$ and H_2O_2 (Isonaka et al. 2011), was shown to induce oxidative damage to both lysosomes and mitochondria. The content of the intralysosomal redox-active iron was suggested as the major determinant in H_2O_2 -induced cell death, and, as supported by our study, its decrease was proposed to be the major mechanism involved in the protective effect of NH_4Cl in cells (Yu et al. 2003). En-

hanced cell death may be an obvious reason of the observed reduced ROS production in contrast to NH_4Cl -exposed cells. However, increase of ROS production and enhanced cell death upon pH gradient disruption by bafilomycin A1 was also observed in BHP-exposed hepatocytes explained by iron relocation from lysosomes to mitochondria (Uchiyama et al. 2008). In this regard, the strong interaction of ammonium chloride with components of the membrane (Petrov et al. 2011) could explain its enhanced stability and lower permeabilisation for EB in NH_4Cl -exposed cells.

Despite its better free radical scavenging efficacy ($-\Delta A/\Delta t = 0.041$) (Rackova et al. 2011) and predicted more effective partitioning into lipid phase ensured by negligible protonation at pH 7.4 (Rackova et al. 2006), EC-STO failed to show a more effective protection of mitochondria, lysosomes and viability of microglial cells against oxidative damage induced by BHP than did STO. In contrast to STO (DR 15.6), EC-STO cannot be successfully accumulated in acidic compartments (DR 1.08). In addition, partial protonation at indolic nitrogen (8.2% participation of $^+NH_2$ form at pH 6, as calculated for pK_{a1} 4.95) can to some extent interfere with its antioxidant action (Steenken et al. 1992).

In support of the hypothetical proton-trap mechanism as a key event in enhanced antioxidant efficacy of STO, its



Scheme 1. Principle of proton-trap mechanism driving accumulation of weakly basic hexahydropyridoindoles within lysosomal space. The concentration gradient of neutral form of the molecule is established across the lysosomal membrane. Portions of unprotonated forms are calculated for $pK_{a2} = 8.5$ of STO (Stefek et al. 1989, using Henderson-Hasselbalch equation: $pH = pK_a + \log ([A^-]/[AH])$). Indolic nitrogen responsible for antioxidant action (Steenken et al. 1992) undergoes negligible protonation: 99.99%, 99.99%, 86.3–99.85% participation of unprotonated form at pH 7.4, 7.2 and 4–6, respectively, calculated for $pK_{a1} = 3.2$ of STO (Stefek et al. 1989) and hence it is available for reaction with free radicals. From plasma (pH 7.4) and cytosol (pH 7.2), a pyridoindole may readily diffuse across membranes in its unprotonated form (while maintaining Henderson-Hasselbalch equilibrium with its ionised form, which cannot readily diffuse across membranes). After diffusion into the acidic compartment of the lysosome (pH 4–6), the equilibrium between charged and uncharged species shifts in favour of the protonated form, limiting diffusion of the drug back into the cytosol and, consequently, trapping the compound in lysosomes. Horizontal arrows correspond to rapid passive diffusion; vertical arrows denote Henderson-Hasselbalch equilibrium.

prevention by the alkalisising agent NH_4Cl eradicated the efficacy STO in suppression of BHP-induced production of H_2DCF -sensitive ROS (i. e. peroxy-, hydroxyl- and alkoxy-radical species (Halliwell and Whiteman 2004)) and cell death induction. In further support of our study, EC-STO was found to be more protective compared to STO in the system of isolated red blood cells oxidatively damaged by BHP (Stefek et al. 2013). Since erythrocytes lack endosomes/lysosomes, the proton trap mechanism cannot contribute to the protection of these cells by STO.

Furthermore, a mild protective efficacy of NT-STO against peroxidative damage and its elimination by proton gradient disruption suggests that this compound (or hexahydropyridindoles generally) can provide stabilisation of lysosomal membrane also *via* antioxidant-action-independent mechanisms. Because of their cationic nature, hexahydropyridindoles might interact with various components of membranes, such as acidic (phospho)lipids or negatively charged residues of membrane-bound proteins, which could affect some properties of these biological barriers. An analogical effect was documented for polyamines and guanidine-compounds bearing protonated amino-groups leading to enhanced stabilisation of various membraneous organelles, including lysosomes (Schuber 1989; Vojtaššák et al. 2008).

Conclusions

In conclusion, our study suggests that weakly basic hexahydropyridindoles (such as STO) may act as lysosomotropic compounds. Furthermore, their weakly basic characteristics (acting as driving force for specific targeting into acidic compartments) may contribute to their improved efficacy in the suppression of peroxidative processes within lysosomes, and thus possibly combating many ageing-related pathologies (Scheme 1). The present study can be considered as mechanistic. The biological effects in the CNS accompanying lysosomotropy may be observed at physiological range of concentrations in case of more lipophilic hexahydropyridindole congeners (particularly N-benzyl-derivatives, Stolc et al. SK-Pat. 287506, 2003). Yet these might be also relevant in case of topical application of STO.

Acknowledgement. In memory of Vladimír Šnirc, a dear friend and bright scientist. This work was supported by VEGA 2/0031/12 and VEGA 1/0076/13.

Conflict of interest: The authors declare no conflict of interest.

References

- Ammoury A., Michaud S., Paul C., Prost-Squarcioni C., Alvarez F., Lamant L., Launay F., Bazex J., Chouini-Lalanne N., Marguery M. C. (2008): Photodistribution of blue-gray hyperpigmentation after amiodarone treatment: molecular characterization of amiodarone in the skin. *Arch. Dermatol.* **144**, 92–96
<http://dx.doi.org/10.1001/archdermatol.2007.25>
- Ashoor R., Yafawi R., Jessen B., Lu S. (2013): The contribution of lysosomotropism to autophagy perturbation. *PLoS One* **8**, e82481
<http://dx.doi.org/10.1371/journal.pone.0082481>
- Blasi E., Barluzzi R., Mazzolla R., Bistoni F. (1990): Immortalization of murine microglial cells by a v-raf/v-myc carrying retrovirus. *J. Neuroimmunol.* **27**, 229–237
[http://dx.doi.org/10.1016/0165-5728\(90\)90073-V](http://dx.doi.org/10.1016/0165-5728(90)90073-V)
- Brunk U. T., Terman A. (2002): The mitochondrial-lysosomal axis theory of aging: accumulation of damaged mitochondria as a result of imperfect autophagocytosis. *Eur. J. Biochem.* **269**, 1996–2002
<http://dx.doi.org/10.1046/j.1432-1033.2002.02869.x>
- Camus P., Mehendale H. M. (1986): Pulmonary sequestration of amiodarone and desethylamiodarone. *J. Pharmacol. Exp. Ther.* **237**, 867–873
- De Mei C., Ercolani L., Parodi C., Veronesi M., Vecchio C. L., Bottegoni G., Torrente E., Scarpelli R., Marotta R., Ruffili R., Mattioli M., Reggiani A., Wade M., Grimaldi B. (2014): Dual inhibition of REV-ERB β and autophagy as a novel pharmacological approach to induce cytotoxicity in cancer cells. *Oncogene* **34**, 2597–2608
- Dickens B. F., Weglicki W. B., Boehme P. A., Mak T. I. (2002): Antioxidant and lysosomotropic properties of acridine-propranolol: protection against oxidative endothelial cell. *J. Mol. Cell. Cardiol.* **34**, 129–137
<http://dx.doi.org/10.1006/jmcc.2001.1495>
- de Duve C., de Barse T., Trouet A., Tulkens P., van Hoof F. (1974): Lysosomotropic agents. *Biochem. Pharmacol.* **23**, 2495–2531
[http://dx.doi.org/10.1016/0006-2952\(74\)90174-9](http://dx.doi.org/10.1016/0006-2952(74)90174-9)
- Gallová J., Szalayová S. (2004): The effect of stobadine on the copper-induced peroxidation of egg yolk phosphatidylcholine in multilamellar liposomes. *Gen. Physiol. Biophys.* **23**, 297–306
- Giulian D., Baker T. J. (1986): Characterization of ameboid microglia isolated from developing mammalian brain. *J. Neurosci.* **6**, 2163–2178
- Halliwell B., Whiteman M. (2004): Measuring reactive species and oxidative damage in vivo and in cell culture: how should you do it and what do the results mean? *British J. Pharmacol.* **142**, 231–255
<http://dx.doi.org/10.1038/sj.bjp.0705776>
- Hiruma H., Kawakami T. (2011): Characteristics of weak base-induced vacuoles formed around individual acidic organelles. *Folia Histochem. Cytobiol.* **49**, 272–279
<http://dx.doi.org/10.5603/FHC.2011.0038>
- Höhn A., Jung T., Grimm S., Catalgol B., Weber D., Grune T. (2011): Lipofuscin inhibits the proteasome by binding to surface motifs. *Free Radic. Biol. Med.* **50**, 585–591
<http://dx.doi.org/10.1016/j.freeradbiomed.2010.12.011>
- Höhn A., Grune T. (2013): Lipofuscin: formation, effects and role of macroautophagy. *Redox. Biol.* **1**, 140–144
<http://dx.doi.org/10.1016/j.redox.2013.01.006>
- Hoss D. M., Gross E. G., Grant-Kels J. M. (1999): Histopathology of an adverse reaction to a eutectic mixture of the local anesthetics lidocaine and prilocaine. *J. Cutan. Pathol.* **26**, 100–104

- <http://dx.doi.org/10.1111/j.1600-0560.1999.tb01810.x>
- Horakova L., Giessauf A., Raber G., Esterbauer H. (1996): Effect of stobadine on Cu(++)-mediated oxidation of low-density lipoprotein. *Biochem. Pharmacol.* **51**, 1277–1282
[http://dx.doi.org/10.1016/0006-2952\(96\)00033-0](http://dx.doi.org/10.1016/0006-2952(96)00033-0)
- Horáková L., Stolc S. (1998): Antioxidant and pharmacodynamic effects of pyridoindole stobadine. *Gen. Pharmacol.* **30**, 627–638
[http://dx.doi.org/10.1016/S0306-3623\(97\)00300-5](http://dx.doi.org/10.1016/S0306-3623(97)00300-5)
- Isonaka R., Hiruma H., Kawakami T. (2011): Inhibition of axonal transport caused by tert-butyl hydroperoxide in cultured mouse dorsal root ganglion neurons. *J. Mol. Neurosci.* **45**, 194–201
<http://dx.doi.org/10.1007/s12031-010-9457-3>
- Jiang P. D., Zhao Y. L., Shi W., Deng X. Q., Xie G., Mao Y. Q., Li Z. G., Zheng Y. Z., Yang S. Y., Wei Y. Q. (2008): Cell growth inhibition, G2/M cell cycle arrest, and apoptosis induced by chloroquine in human breast cancer cell line Bcap-37. *Cell. Physiol. Biochem.* **22**, 431–440
<http://dx.doi.org/10.1159/000185488>
- Juranek I., Rackova L., Stefek M. (2012): Stobadine – an indole type alternative to the phenolic antioxidant reference trolox. In: *Biochemistry*. (Ed. D. Ekinici), pp. 443–452 InTech, Rijeka
<http://dx.doi.org/10.5772/32784>
- Korolchuk V. I., Menzies F.M., Rubinsztein D. C. (2010): Mechanisms of cross-talk between the ubiquitin-proteasome and autophagy-lysosome systems. *FEBS Lett.* **584**, 1393–1398
<http://dx.doi.org/10.1016/j.febslet.2009.12.047>
- Kramer J. H., Murthi S. B., Wise R. M., Mak I. T., Weglicki W. B. (2006): Antioxidant and lysosomotropic properties of acute D-propranolol underlies its cardioprotection of postischemic hearts from moderate iron-overloaded rats. *Exp. Biol. Med.* **231**, 473–484
- Kyselova Z., Rackova L., Stefek M. (2003): Pyridoindole antioxidant stobadine protected bovine serum albumin against the hydroxyl radical mediated cross-linking in vitro. *Arch. Gerontol. Geriatr.* **36**, 221–229
[http://dx.doi.org/10.1016/S0167-4943\(02\)00167-X](http://dx.doi.org/10.1016/S0167-4943(02)00167-X)
- Liu B., Wang K., Gao H. M., Mandavilli B., Wang J. Y., Hong J. S. (2001): Molecular consequences of activated microglia in the brain: overactivation induces apoptosis. *J. Neurochem.* **77**, 182–189
<http://dx.doi.org/10.1046/j.1471-4159.2001.t01-1-00216.x>
- Marceau F., Bawolak M. T., Lodge R., Bouthillier J., Gagné-Henley A., Gaudreault R. C., Morissette G. (2012): Cation trapping by cellular acidic compartments: beyond the concept of lysosomotropic drugs. *Toxicol. Appl. Pharmacol.* **259**, 1–12
<http://dx.doi.org/10.1016/j.taap.2011.12.004>
- Mariani E., Polidori M. C., Cherubini A., Mecocci P. J. (2005): Oxidative stress in brain aging, neurodegenerative and vascular diseases: an overview. *Chromatogr. B Analyt. Technol. Biomed. Life Sci.* **827**, 65–75
<http://dx.doi.org/10.1016/j.jchromb.2005.04.023>
- Majumdar A., Cruz D., Asamoah N., Buxbaum A., Sohar I., Lobel P., Maxfield F. R. (2007): Activation of microglia acidifies lysosomes and leads to degradation of alzheimer amyloid fibrils. *Mol. Biol. Cell* **18**, 1490–1496
<http://dx.doi.org/10.1091/mbc.E06-10-0975>
- MarvinSketch 6.3.1, 2014, ChemAxon (<http://www.chemaxon.com>), Calculator Plugins were used for structure property prediction and calculation
<http://dx.doi.org/10.1038/onc.2014.203>
- Milackova I., Rackova L., Majekova M., Mrvova N., Stefek M. (2015): Protection or cytotoxicity mediated by a novel quinonoid-polyphenol compound? *Gen. Physiol. Biophys.* **34**, 51–64
http://dx.doi.org/10.4149/gpb_2014028
- Navarová J., Macicková T., Horáková K., Urbancíková M. (1999): Stobadine inhibits lysosomal enzyme release in vivo and in vitro. *Life Sci.* **65**, 1905–1907
[http://dx.doi.org/10.1016/S0024-3205\(99\)00445-2](http://dx.doi.org/10.1016/S0024-3205(99)00445-2)
- Pallas Version 3.1.1.2, CompuDrug International, 115 Morgan Dr., Sedona, AZ 86351
- Persson H. L., Yu Z., Tirosh O., Eaton J. W., Brunk U. T. (2003): Prevention of oxidant-induced cell death by lysosomotropic iron chelators. *Free Radic. Biol. Med.* **34**, 1295–1305
[http://dx.doi.org/10.1016/S0891-5849\(03\)00106-0](http://dx.doi.org/10.1016/S0891-5849(03)00106-0)
- Persson H. L., Vainikka L. K., Sege M., Wennerström U., Dam-Larsen S., Persson J. (2012): Leaky lysosomes in lung transplant macrophages: azithromycin prevents oxidative damage. *Respir. Res.* **13**, 83
<http://dx.doi.org/10.1186/1465-9921-13-83>
- Petrov M., Cwiklik L., Jungwirth P. (2011): Interactions of molecular ions with model phospholipid membranes. *Coll. Czech. Chem. Commun.* **76**, 695–711
<http://dx.doi.org/10.1135/cccc2011026>
- Rackova L., Stefek M., Majekova M. (2002): Structural aspects of antioxidant activity of substituted pyridoindoles. *Redox Rep.* **7**, 207–214
<http://dx.doi.org/10.1179/135100002125000578>
- Rackova L., Snirc V., Majekova M., Majek P., Stefek M. (2006): Free radical scavenging and antioxidant activities of substituted hexahydropyridoindoles. Quantitative structure-activity relationships. *J. Med. Chem.* **49**, 2543–2548
<http://dx.doi.org/10.1021/jm060041r>
- Ráčková L., Šnirc V., Jung T., Štefek M., Karasu Ç., Grune T. (2009): Metabolism-induced oxidative stress is a mediator of glucose toxicity in HT22 neuronal cells. *Free Radic. Res.* **43**, 876–886
<http://dx.doi.org/10.1080/10715760903104374>
- Ráčková L., Cumaoglu A., Bağriacik E.U., Štefek M., Maechler P., Karasu Ç. (2011): Novel hexahydropyridoindole derivative as prospective agent against oxidative damage in pancreatic β cells. *Med. Chem.* **7**, 711–717
<http://dx.doi.org/10.2174/157340611797928370>
- Ribble D., Goldstein N. B., Norris D. A., Shellman Y. G. (2005): A simple technique for quantifying apoptosis in 96-well plates. *BMC Biotechnol.* **5**, 12
<http://dx.doi.org/10.1186/1472-6750-5-12>
- Roy A., Ganguly A., Dasgupta S. B., Das B. B., Pal Ch., Jaisankar P., Majumder H. K. (2008): Mitochondria-dependent reactive oxygen species-mediated programmed cell death induced by 3,3'-diindolylmethane through inhibition of F0F1-ATP synthase in unicellular protozoan parasite *Leishmania donovani*. *Mol. Pharmacol.* **74**, 1292–1307
<http://dx.doi.org/10.1124/mol.108.050161>

- Schuber F. (1989): Influence of polyamines on membrane functions. *Biochem. J.* **260**, 1–10
- Steenken S., Sunquist A. R., Jovanovic S. V., Crockett R., Sies H. (1992): Antioxidant activity of the pyridoindole stobadine. Pulse radiolytic characterization of one-electron-oxidized stobadine and quenching of singlet molecular oxygen. *Chem. Res. Toxicol.* **5**, 355–360
<http://dx.doi.org/10.1021/tx00027a006>
- Stefek M., Benes L., Zelnik V. (1989): N-oxygenation of stobadine, a gamma-carboline antiarrhythmic and cardioprotective agent: the role of flavin-containing monooxygenase. *Xenobiotica* **19**, 143–150
<http://dx.doi.org/10.3109/00498258909034686>
- Stefek M., Drozdikova I., Vajdova K. (1996): The pyridoindole anti-oxidant stobadine inhibited glycation-induced absorbance and fluorescence changes in albumin. *Acta Diabetol.* **33**, 35–40
<http://dx.doi.org/10.1007/BF00571938>
- Stefek M., Milackova I., Juskova-Karasova M., Snirc V. (2013): Antioxidant action of the hexahydropyridoindole SMe1EC2 in the cellular system of isolated red blood cells in vitro. *Redox Rep.* **18**, 71–75
<http://dx.doi.org/10.1179/1351000213Y.0000000043>
- Štolc S., Považanec F., Bauer V., Májejková M., Wilcox A. L., Šnirc V., Račková L., Sotníková R., Štefek M., Gáspárová Z., Gajdošíková A., Mihalová D., Alfoldi J. (2005): SK-Pat. 287506, Patent Appl. 1321–2003
- Sundelin S. P., Terman A. (2002): Different effects of chloroquine and hydroxychloroquine on lysosomal function in cultured retinal pigment epithelial cells. *APMIS* **110**, 481–489
<http://dx.doi.org/10.1034/j.1600-0463.2002.100606.x>
- Tremblay M.-È., Stevens B., Sierra A., Wake H., Bessis A., Nimmerjahn A. (2011): The role of microglia in the healthy brain. *J. Neurosci.* **31**, 16064–160649
<http://dx.doi.org/10.1523/JNEUROSCI.4158-11.2011>
- Uchiyama A., Kim J.-S., Kon K., Jaeschke H., Ikejima K., Watanabe S., Lemasters J. J. (2008): Translocation of iron from lysosomes into mitochondria is a key event during oxidative stress-induced hepatocellular injury. *Hepatology* **48**, 1644–1654
<http://dx.doi.org/10.1002/hep.22498>
- Vandenbroucke-Grauls C. M., Thijssen R. M., Marcelis J. H., Sharma S. D., Verhoef J. (1984): Effects of lysosomotropic amines on human polymorphonuclear leucocyte function. *Immunology* **51**, 319–326
- Vojtaššák J., Blaško Sr. M., Danišovič L., Čársky J., Ďuríková M., Repiska V., Waczulíkova I., Böhmer D. (2008): In vitro evaluation of the cytotoxicity and genotoxicity of resorcylic-dene aminoguanidine in human diploid cells B-HNF-1. *Folia Biologica* **54**, 109–114.
- Wong W. T. (2013): Microglial aging in the healthy CNS: phenotypes, drivers, and rejuvenation. *Front. Cell. Neurosci.* **7**, 22
<http://dx.doi.org/10.3389/fncel.2013.00022>
- Wong P. Y. Y., Kitts D. D. (2001): An iron binding assay to measure activity of known food sequestering agents: studies with buttermilk solids. *Food Chem.* **72**, 245–254
[http://dx.doi.org/10.1016/S0308-8146\(00\)00237-5](http://dx.doi.org/10.1016/S0308-8146(00)00237-5)
- Yayon A., Cabantchik Z. I., Ginsburg H. (1985): Susceptibility of human malaria parasites to chloroquine is pH dependent. *Proc. Nat. Acad. Sci. USA* **82**, 2784–2788
<http://dx.doi.org/10.1073/pnas.82.9.2784>
- Yu Z., Persson H. L., Eaton J. W., Brunk U. T. (2003) Intralysosomal iron: a major determinant of oxidant-induced cell death. *Free Radic. Biol. Med.* **34**, 1243–1252
[http://dx.doi.org/10.1016/S0891-5849\(03\)00109-6](http://dx.doi.org/10.1016/S0891-5849(03)00109-6)

Received: February 28, 2015

Final version accepted: May 15, 2015

First published online: July 29, 2015